Journal of Pharmaceutical Analysis 7 (2017) 19–26

Contents lists available at ScienceDirect

Journal of Pharmaceutical Analysis

journal homepage: www.elsevier.com/locate/jpa

Original Research Article

Binding interaction of phosphorus heterocycles with bovine serum albumin: A biochemical study

Swarup Roy[a], Raj Kumar Nandi[b], Sintu Ganai[b], K.C. Majumdar[b,*], Tapan K. Das[a,*]

[a] Department of Biochemistry and Biophysics, University of Kalyani, Kalyani 741235, West Bengal, India
[b] Department of Chemistry, University of Kalyani, Kalyani 741235, West Bengal, India

ARTICLE INFO

Keywords:
BSA
Spectroscopy
Phosphorus heterocycles
BSA-PHs docking

ABSTRACT

Interaction between bovine serum albumin (BSA) and phosphorus heterocycles (PHs) was studied using multi-spectroscopic techniques. The results indicated the high binding affinity of PHs to BSA as it quenches the intrinsic fluorescence of BSA. The experimental data suggested the fluorescence quenching mechanism between PHs and BSA as a dynamic quenching. From the UV–vis studies, the apparent association constant (K_{app}) was found to be 9.25×10^2, 1.27×10^4 and 9.01×10^2 L/mol for the interaction of BSA with PH-1, PH-2 and PH-3, respectively. According to the Förster's non-radiation energy transfer (FRET) theory, the binding distances between BSA and PHs were calculated. The binding distances (r) of PH-1, PH-2 and PH-3 were found to be 2.86, 3.03, and 5.12 nm, respectively, indicating energy transfer occurs between BSA and PHs. The binding constants of the PHs obtained from the fluorescence quenching data were found to be decreased with increase of temperature. The negative values of the thermodynamic parameters ΔH, ΔS and ΔG at different temperatures revealed that the binding process is spontaneous; hydrogen bonds and van der Waals interaction were the main force to stabilize the complex. The microenvironment of the protein-binding site was studied by synchronous fluorescence and circular dichroism (CD) techniques and data indicated that the conformation of BSA changed in the presence of PHs. Finally, we studied the BSA-PHs docking using AutoDock and results suggest that PHs is located in the cleft between the domains of BSA.

1. Introduction

Bovine serum albumin (BSA), a single-chain globular nonglycoprotein, consists of 583 amino acid residues and comprises three structurally homologous domains (I-III) that are divided into nine loops (L1-L9) by 17 disulfide bonds. Like most abundant proteins in the circulatory system, BSA acts as a transporter and distributor of many endogenous and exogenous compounds. BSA has physiological functions involving the binding, transport, and delivery of fatty acids, bilirubin, porphyrins, thyroxine, tryptophan, and steroids. It is also able to bind metals, pharmaceuticals, and drugs at specific binding sites. Binding of drugs to plasma proteins is an important pharmacological characteristic, because strong albumin binding diminishes the active concentration of a drug in plasma. This leads to competitive release of other drugs that may be bound to albumin, and which may be administered during the same time frame [1]. The subsequent increase in the concentration of the released drug may lead to serious drug-drug interactions. Besides, a very high affinity of potential drug molecules for BSA is usually undesirable [2]. Studies on protein-drug interactions may provide information of the structural features that determine the therapeutic effectiveness of the drugs. Therefore, the study of interactions between BSA and potential molecules is an important field of research in life science, chemistry, and clinical medicine [3].

On the other hand, phosphorus containing heterocyclic compounds is known to be used as a catalytic antibody as well as an anti-cancer agent [4]. These derivatives are also known to be anti-hypertensive agents [5]. It is widely accepted that the distribution, metabolism, and efficacy of many drugs can be altered based on their affinity to serum albumin [6]. The knowledge of the interaction and binding to BSA provides information on the pharmacological action of phosphorus containing heterocyclic compounds and illuminates its binding mechanism.

There have been several studies on the fluorescence quenching of proteins induced by some compounds with different substituents. Already in recent years few reports have been published regarding interaction between serum albumin and synthetic organic compounds [7–9]. Very recently, the interaction between novel spiro[cyclopropane-pyrrolizin] and BSA has been studied by Yu et al. [10]. Wang et al.

Peer review under responsibility of Xi'an Jiaotong University.
* Corresponding authors.
E-mail addresses: kcmklyuniv@gmail.com (K.C. Majumdar), tapankumardas175@gmail.com (T.K. Das).

http://dx.doi.org/10.1016/j.jpha.2016.05.009
Received 16 February 2016; Received in revised form 24 May 2016; Accepted 30 May 2016
Available online 15 June 2016

[11] reported the interaction between clenbuterol hydrochloride and BSA. The interaction between orientin and BSA was investigated by Toprak et al. [12]. Roy et al. [13–15] described the interaction of pyrimidine-annulated spiro-dihydrofuran, spirooxindole annulated thiopyran derivatives, and pyrano [3, 2-f] quinoline derivatives with BSA. Yao et al. [16] reported the study of interaction between carteolol hydrochloride and urea induced BSA and also interaction of phacolysin with BSA was reported by Yu et al. [17]. Hu et al. [18] reported the interaction between anti-tumor drugs, 1-hexylcarbamoyl-5-fluorouracil (carmofur) and BSA using multi-spectroscopic approach. Zhang et al. [19] reported interaction of cefixime (CFX) with BSA by fluorescence quenching spectroscopy and synchronous fluorescence spectroscopy. Dutta et al. [20] described the interaction between diclofenac sodium and BSA. Wang et al. [21] showed the interaction of efonidipine with BSA. Nafisi et al. [22] reported interaction of aspirin with BSA.

To the best of our knowledge, there is no report on the interaction of phosphorous heterocycles (PHs) with BSA. In order to determine the affinity of PHs to BSA, we investigated the thermodynamics of their interaction using fluorescence spectroscopy. We also used circular dichroism (CD) technique to investigate any structural modification of biomolecules in the presence of PHs. Determination of the distances between BSA as donor and PHs as acceptors was also carried out according to the Förster's energy transfer theory. Moreover, molecular modeling was used to improve the understanding of the interaction of PHs with BSA.

2. Materials and methods

2.1. Materials

The phosphorous heterocycles (PHs) required for our study were prepared according to published procedure using ring closing metathesis reaction [23]. Here, PH-1 is a uracil annulated oxophosphocine derivative whereas PH-2 and PH-3 are differently substituted benzooxophosphocine derivatives. The unsymmetrical alkenyl substrates (P-1, P-2, P-3) were treated with 5 mol% Grubbs' Cat I in dichloromethane (CH_2Cl_2) under a nitrogen atmosphere at room temperature for 5 h and the corresponding 8-membered PHs (PH-1, PH-2, PH-3) were obtained in excellent yield (Scheme 1). The crude products were purified using chromatographic separation techniques.

Bovine serum albumin (BSA; Sigma, USA) was used in this experiment. The stock solution of BSA was prepared by dissolving BSA in a Tris–HCl buffer (50 mM, PH 7.4) to make the concentration as 0.1 μM. Synthesized PHs were dissolved in methanol (1 mM). All the other chemicals were of analytical reagent grade and double distilled water was used.

2.2. Apparatus

Fluorescence spectra were recorded on Cary-Eclipse Fluorescence Spectrophotometer (Agilent Technologies, Australia), well equipped with an attached Cary Temperature Controller. The absorption spectra were obtained by using Cary series UV–vis spectrophotometer (Agilent Technologies, Australia). CD spectra were analyzed by a Jasco J-815 CD spectrometer, Japan.

2.3. Methods

2.3.1. UV–visible spectroscopy

The absorption titration was performed by keeping the concentration of BSA at 0.1 μM, meanwhile varying the PHs concentration (0–25 μM). The absorption spectra were recorded from 230 to 330 nm at room temperature (303 K). The absorption spectra were checked above 330 nm but were not reported as there were no significant changes above this region. All the experiments were performed in Tris–HCl buffer (50 mM, PH 7.4) in a conventional quartz cell.

2.3.2. Intrinsic fluorescence

0.1 μM BSA solution (3 mL) was titrated by successive additions of PHs (0–30 μM). Fluorescence spectra were recorded in the range of 300–450 nm at the excitation wavelength of 279 nm. The fluorescence spectra were recorded at four different temperatures (293, 298, 303 and 313 K). The range of synchronous scanning was λ_{ex}=240 nm to λ_{em}=255 nm, where the difference in the wavelength (Δλ) was 15 nm,

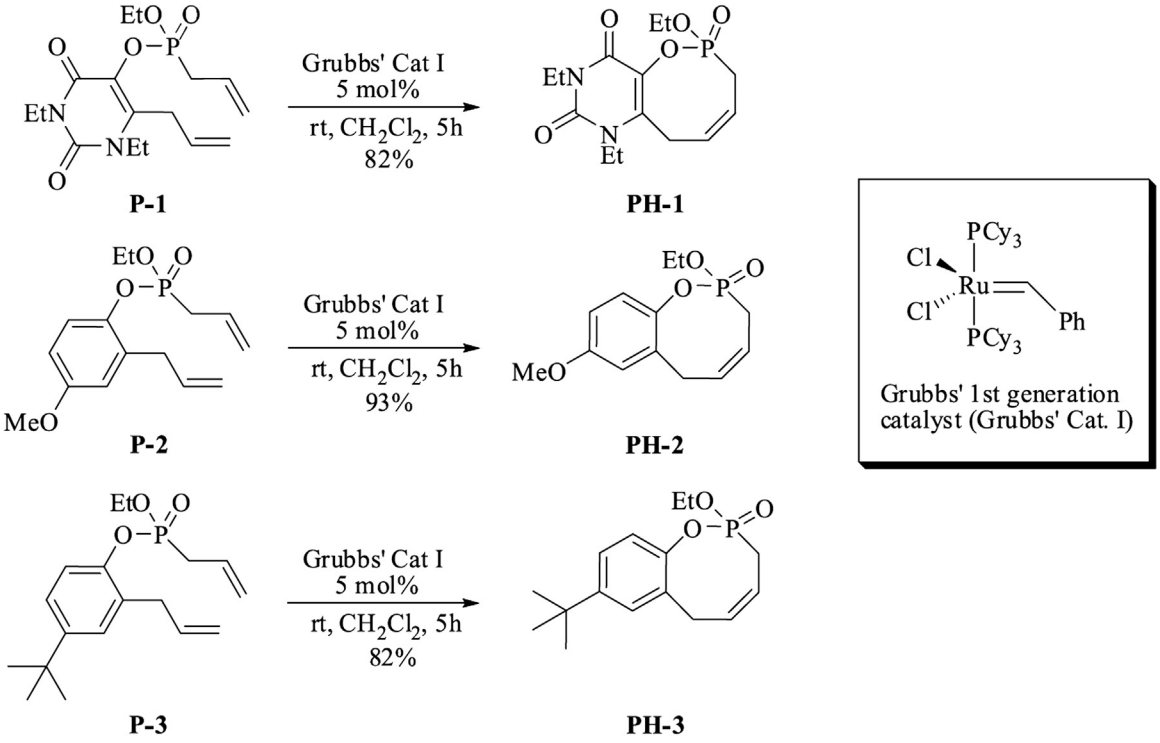

Scheme 1. Synthesis of phosphorous containing heterocycles by ring closing metathesis (RCM).

and λ_{ex}=240 nm to λ_{em}=300 nm, where the difference in the wavelength (Δλ) was 60 nm.

2.3.3. Circular dichroism spectra

The far-UV CD region (190–260 nm), which corresponds to peptide bond absorption, was analyzed in a CD spectrometer to give the content of the regular secondary structure in BSA. Protein solutions were prepared in Tris–HCl buffer (50 mM, PH 7.4). Protein solutions of 0.01 μM were used to record the spectra. Spectral changes of BSA were monitored after adding different concentration of PHs (0–25 μM).

2.3.4. Molecular docking

The crystal structure of BSA used was from the Protein Data Bank (entry code 4F5S). The Auto Dock 4.0 was employed to compute the possible binding mode of PHs with BSA. The 3D structures of PHs and BSA were modeled on molecular modeling software Discovery Studio 4.0. The docking calculations were then performed using the Lamarckian genetic algorithm (LGA) for ligand conformational searching. LGA implemented in the AutoDock was used to estimate the possible binding conformations of PHs. During the docking process, a maximum of 10 different conformations were considered for PHs. The conformer with the lowest binding free energy was used for further analysis.

3. Results and discussion

3.1. Absorption characteristics of BSA-PHs interaction

To find out the specific molecular interaction between PHs and BSA, the absorption spectra of BSA were monitored in the absence or presence of PHs. Fig. 1 shows the absorption spectra of BSA and BSA in the presence of increasing concentration of PH-1. It was found that with increase of PHs concentration the absorption intensity at wavelength 279 nm increased continuously with a significant red shift of the peak maxima. The shift in wavelength at 279 nm suggested the change in hydrophobicity of BSA molecules.

This increase in intensity may be due to the formation of the ground state complex between BSA and PH-1. In order to compare quantitatively the binding strength of PHs, the apparent association constants K_{app} of PHs with BSA were obtained by monitoring the changes in absorbance of BSA at 279 nm. The equilibrium for the formation of complex between BSA and PHs is given by the Eq. (1) and the values of the K_{app} were obtained from the BSA absorption data at 279 nm according to the published method [24]. The K_{app} values were calculated based on Benesi and Hildebrand equation [25].

$$\frac{1}{A_{obs} - A_0} = \frac{1}{A_c - A_0} + \frac{1}{K_{app}(A_c - A_0)[PHs]} \quad (1)$$

Here A_0 is the absorbance of BSA in the absence of PH-1 and A_C is the recorded absorbance at 279 nm for BSA at different PH-1 concentrations. The double reciprocal plot of $1/(A_{obs}-A_0)$ vs 1/[PHs] was linear and K_{app} was estimated to be 9.25×10^2 L/mol (R=0.9969, where R is the correlation coefficient) (Fig. 1 inset) from the ratio of the intercept to the slope [24]. In case of PH-2 and PH-3, K_{app} values were 1.27×10^4 and 9.01×10^2 L/mol (R = 0.9987 and 0.9994 for PH-2 and PH-3), respectively. UV–vis spectra of PH-2 and PH-3 are shown in Supplementary Fig. 1. The value of K_{app} was considerably small, thereby indicating formation of a weak complex between BSA and PHs. The UV–vis spectra of the compounds PH-1, PH-2 and PH-3 are shown in Supplementary Fig. 2. From the graph it was observed that PHs has absorption peak in the range of 270–280 nm. Also the spectral differences between BSA (0.1 μM), PHs (5 μM) and BSA+PHs are shown in Supplementary Fig. 2. From the figure it was clearly observed that absorption intensity of BSA increases in the presence of PHs.

3.2. Characteristics of fluorescence spectra

Fluorescence of BSA mainly originates from tryptophan, tyrosine, and phenylalanine residues, whereas the intrinsic fluorescence of BSA is mainly contributed by the tryptophan residues. An important feature of the intrinsic fluorescence of the protein is the high sensitivity of tryptophan to its local environment [26]. Changes in emission spectra of tryptophan are common in response to protein conformational transitions, subunit association, substrate binding, or denaturation [27]. Therefore, the intrinsic fluorescence of proteins can provide significant information about their structures and dynamics.

The fluorescence characteristics of serum albumins are very sensitive to its microenvironment [27,28]. To further investigate the interactions of the PHs with BSA, fluorescence quenching measurements were performed. The fluorescence emission spectra of BSA and BSA titrated with PH-1 are shown in Fig. 2. It can be observed that with the increase of PH-1 concentration the emission intensity decreased. In case of PH-2 and PH-3, similar sort of results were observed, which are shown in Supplementary Fig. 3. The emission spectra of the compounds PH-1, PH-2 and PH-3 were also shown in Supplementary Fig. 4 and it was observed that PHs has emission peak in the range of 295–325 nm upon excitation at 280 nm.

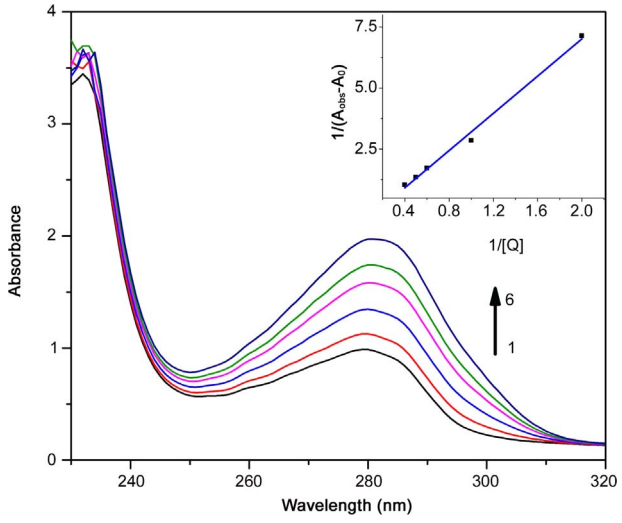

Fig. 1. Absorption spectra of BSA (0.1 μM) in presence of PH-1 (0, 5, 10, 15, 20 and 25 μM). The inset shows calculation of K_{app} of BSA-PH-1 complex; $1/(A_{obs}-A_0)$ vs 1/[PH-1] plot.

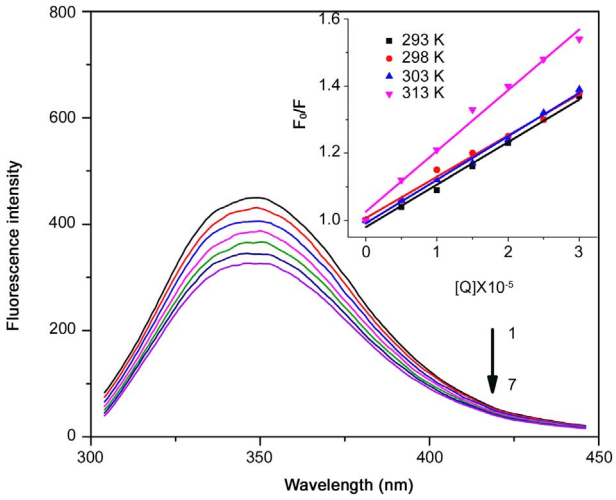

Fig. 2. Fluorescence quenching spectra of BSA in presence of PH-1. The inset shows the Stern-Volmer plot for PH-1 and BSA at 293, 298, 303, and 313 K, respectively.

Fluorescence quenching is usually classified as either dynamic quenching or static quenching. Dynamic quenching occurs when excited state fluorophores are deactivated upon contacting with the quencher molecule in solution. Static quenching occurs by the formation of a non-fluorescent ground state complex between the fluorophores and the quencher. The dynamic quenching constant increases with increased temperature. However, for static quenching, the quenching constant diminishes with the increase of temperature [29]. The quenching data can be obtained from the following Stern-Volmer equation [29,30].

$$F_0/F = 1 + K_q\tau_0[Q] = 1 + K_{SV}[Q] \quad (2)$$

where F_0 and F represent the fluorescence intensities in the absence and presence of a quencher, K_q is the bimolecular quenching rate constant, K_{SV} is the Stern-Volmer constant, τ_0 is the average lifetime of the molecule without quencher, and [Q] is the concentration of the quencher. Since the fluorescence lifetime of protein is 10^{-8} s [29], the K_q values were calculated using the formula $K_q=K_{SV}/\tau_0$. The maximum scatter quenching collision constant of various quenchers with the biopolymer is near 2×10^{10} L/mol/s in case of dynamic quenching [29]. Quenching data can be presented as plots of F_0/F vs [Q], as F_0/F is expected to be linearly dependent upon the concentration of the quencher. The curves show good linearity within the concentrations investigated at different temperatures. A plot of F_0/F vs [Q] yields a slope equal to Stern-Volmer quenching constant and the results are presented in Table 1 along with the correlation coefficients (*R*). The linearity of the F_0/F vs [Q] plots is shown in Fig. 2 inset. The values of K_q are lower than the maximum diffusion collision quenching rate constant (2×10^{10} L/mol/s). This indicates that the dynamic quenching may exist between PHs and BSA. From the Table 1 it can be seen that the quenching constant of all the three compounds increases with the rise of temperature. This implies that the probable quenching mechanism of BSA is a dynamic quenching process [31–33].

3.3. Binding constant and number of binding sites

The data of fluorescence intensities were analyzed using the Eq. (3) as a hypothetical dynamic quenching process. The binding constant and the number of binding site between the PHs and BSA were estimated by the following equation [34].

$$log\frac{F_0 - F}{F} = \log K + n \log [Q] \quad (3)$$

A plot of log [(F_0–F)/F] vs log [Q] makes a straight line, whose slope equals n and the length of intercept on Y-axis equals log K. Fig. 3 shows the double-logarithm plot (log[(F_0–F)/F] vs log[Q]) and the binding constant, K and number of binding sites, n were obtained at various temperatures and Table 2 gives the corresponding results. For

Table 1
The Stern-Volmer constants and quenching constants of BSA by PHs at varying temperatures.

Compound	Temperature (K)	K_{SV} (L/mol)×10^{-2}	K_q (L/mol/s)×10^6	*R*[a]
PH-1	293	12.6	12.6	0.9959
PH-2	293	10.3	10.3	0.9960
PH-3	293	48.9	48.9	0.9938
PH-1	298	12.3	12.3	0.9961
PH-2	298	10.0	10.0	0.9967
PH-3	298	49.6	49.6	0.9936
PH-1	303	12.9	12.9	0.9975
PH-2	303	10.6	10.6	0.9980
PH-3	303	50.0	50.0	0.9970
PH-1	313	18.0	18.0	0.9940
PH-2	313	13.3	13.3	0.9930
PH-3	313	52.8	52.8	0.9964

[a] Correlation coefficient.

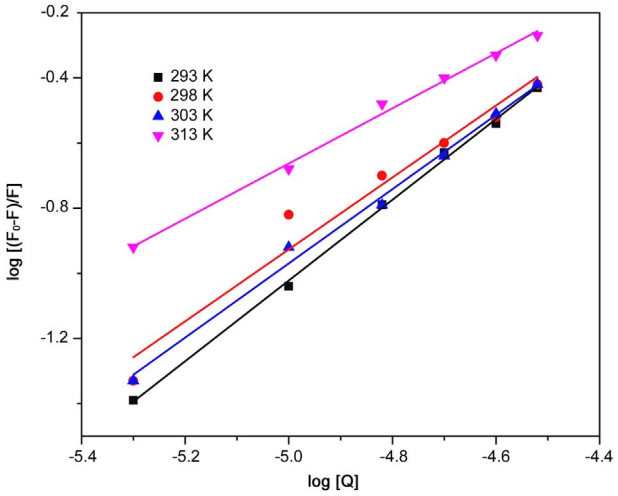

Fig. 3. Plots of the pH-1 quenching effect on BSA fluorescence at 293, 298, 303, and 313 K.

Table 2
Binding constants (K) and the number of binding sites (n) of BSA by PHs at different temperatures.

Compound	Temperature (K)	K (L/mol)×10^4	n	*R*[a]
PH-1	293	18.62	1.24	0.9990
PH-2	293	2.95	1.10	0.9972
PH-3	293	77.60	1.26	0.9993
PH-1	298	3.98	1.10	0.9966
PH-2	298	1.15	1.01	0.9967
PH-3	298	41.70	1.20	0.9990
PH-1	303	5.01	1.14	0.9961
PH-2	303	0.71	0.96	0.9995
PH-3	303	22.90	1.14	0.9987
PH-1	313	0.39	0.85	0.9970
PH-2	313	0.25	0.83	0.9955
PH-3	313	11.48	1.07	0.9985

[a] Correlation coefficient.

PH-2 and PH-3, double-logarithm curve are shown in Supplementary Fig. 5. The values of n at the experimental temperatures were approximately equal to one, which indicates that there is a single binding site in BSA with PHs.

Results of Table 2 indicate that the binding of BSA with PHs is remarkable and the effect of temperature, ranging from 293 K to 313 K, on the binding constant is also noticeable. Similar results considering novel spiro[cyclopropane-pyrrolizin]-BSA system was reported by Yu et al. [10]. The binding constants of the interaction between PHs and BSA increase in the following order: PH-2 < PH-1 < PH-3, i.e., the compound PH-3 has the strongest ability to bind with BSA and compound PH-2 is the weakest. From Table 2, can be seen that with increase in temperature, the binding constant K decreases, which indicates that the stability of the BSA-PHs complexes decreases with the increased temperature.

3.4. Thermodynamic parameters and nature of binding forces

Four types of interactions between a small molecule and a macromolecule are usually known[35], namely H-bond, van der Waals interactions, electrostatic forces and hydrophobic interactions. In general, ΔG reflects the spontaneity of reaction, while ΔH and ΔS are the main quantities for judging the binding force [36,37].

If the enthalpy change does not vary significantly over the temperature range studied, the thermodynamic parameters of ΔH and ΔS can be determined using the Van't Hoff equation (Eq. (4)). Here, ΔH and ΔS were calculated from Van't Hoff plots, shown in Fig. 4, where K

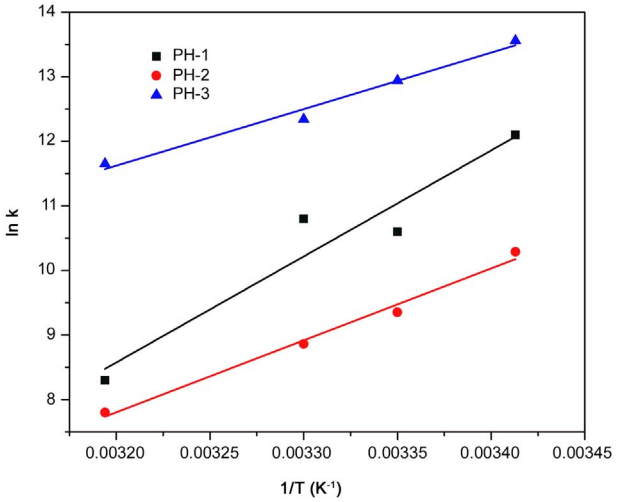

Fig. 4. The Van't Hoff plot for the interaction of BSA and PHs.

is the effective binding constant at the corresponding temperature and R is the gas constant. The Gibbs free energy was estimated from the Eq. (5).

$$\ln K = -\Delta H/RT + \Delta S/R \quad (4)$$

$$\Delta G = \Delta H - T\Delta S = -RT \ln K \quad (5)$$

According to Ross's opinion [38], the sign and magnitude of the thermodynamic parameter are associated with various individual kinds of interaction that may take place in protein association processes. From the thermodynamic standpoint, $\Delta H > 0$ and $\Delta S > 0$ imply a hydrophobic interaction, $\Delta H < 0$ and $\Delta S < 0$ reflect the van der Waals force or hydrogen bond formation. The values of $\Delta H < 0$ and $\Delta S > 0$, indicate the presence of electrostatic force of attraction.

The values of thermodynamic parameters are listed in Table 3. As shown in Table 3 in all the three cases ΔG, ΔH, and ΔS are negative. The negative values of ΔH and ΔS indicate that the binding is mainly enthalpy driven, and the entropy is unfavorable for it. According to previous reports [38,39], the negative ΔH and ΔS values of the interactions of PHs with BSA suggest that the binding process is mainly driven by van der Waals force and hydrogen bond. The negative value of ΔG indicates that the interaction process is spontaneous. Accordingly, it is likely that weak forces are responsible in the binding process. Earlier similar observations were also reported by other groups [7,40,41]. The forces between the novel spiro[cyclopropane-pyrrolizin]-BSA system were also found to be mainly H-bonds and van der Waals interactions according to Yu et al. [10].

Table 3
Thermodynamic parameters for the binding of the PHs with BSA at different temperature.

Compound	Temperature (K)	ΔH (kJ/mol)	ΔS (J/mol/K)	ΔG (kJ/mol)
PH-1	293	−136.51	−365.57	−29.39
PH-2	293	−92.61	−231.46	−24.79
PH-3	293	−72.77	−132.26	−32.85
PH-1	298	−136.51	−365.57	−27.56
PH-2	298	−92.61	−231.46	−23.63
PH-3	298	−72.77	−132.26	−32.17
PH-1	303	−136.51	−365.57	−25.74
PH-2	303	−92.61	−231.46	−22.47
PH-3	303	−72.77	−132.26	−31.49
PH-1	313	−136.51	−365.57	−22.08
PH-2	313	−92.61	−231.46	−20.16
PH-3	313	−72.77	−132.26	−30.12

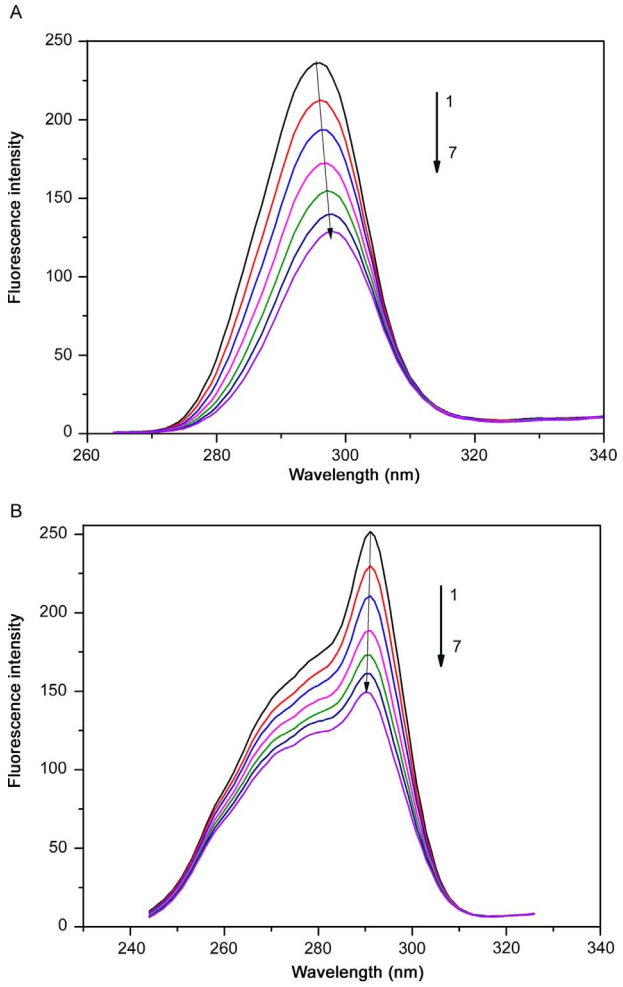

Fig. 5. Synchronous fluorescence spectra of BSA in presence of PH-1 using (A) Δλ=15 nm (λ_{ex}=240 nm, λ_{em}=255 nm) and (B) Δλ=60 nm (λ_{ex}=240 nm, λ_{em}=300 nm).

3.5. Synchronous fluorescence spectra

Synchronous fluorescence spectroscopy has several advantages and is a sensitive technique to analyze the microenvironmental changes of chromospheres [42]. The advantages include sensitivity, spectral simplification, spectral bandwidth reduction and devoid of different perturbing effects. A synchronous fluorescence spectrum gives the information on the molecular environment of the fluorophores functional group. The value of Δλ, i.e., difference between excitation and emission, is an important operating parameter.

According to literature [43,44], synchronous fluorescence spectrum indicates the changes in the microenvironment of tyrosine residues when Δλ=15 nm, and the same for tryptophan residues when Δλ=60 nm. Fig. 5A shows that when Δλ=15 nm there is a clear red shift in the emission wavelength of tyrosine residues. When Δλ=60 nm, no characteristic changes in emission wavelength of tryptophan are observed (Fig. 5B). The red shift in the emission maxima of mainly tyrosine indicates that the polarity around tyrosine residues is increased and the hydrophobicity is decreased in the presence of PH-1 [45]. These results suggested that PH-1 induces a conformational change in BSA. A similar result was also found with PH-2 but in case of PH-3 instead of red shift, blue shift is observed and results are shown in Supplementary Fig. 6.

3.6. Circular dichroism spectroscopy

The CD spectra of BSA exhibited two negative minima at 208 nm and 222 nm, which is characteristics of the helix structure of this class

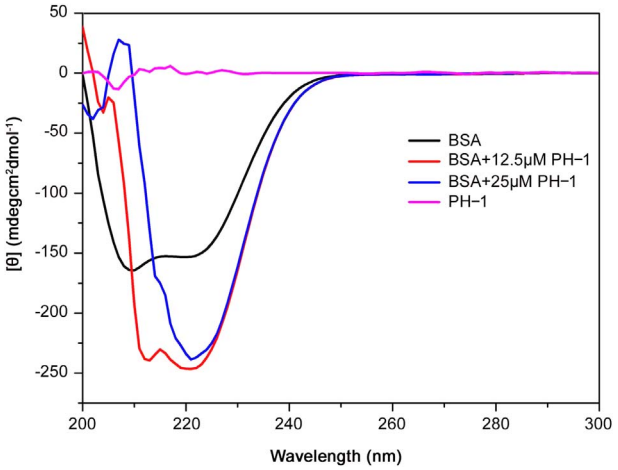

Fig. 6. UV-CD spectra of PH-1 and PH-1-BSA system at the BSA concentration of 0.01 μM and PH-1 concentrations of 0, 12.5 and 25 μM.

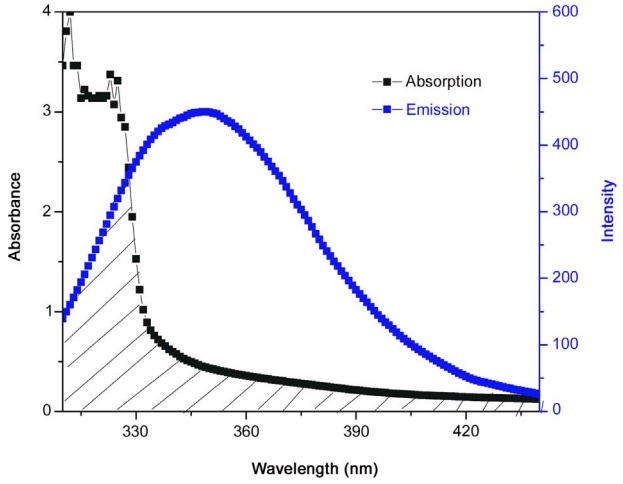

Fig. 7. The overlap plot of the fluorescence emission spectra of BSA (0.1 μM) and the UV absorption spectra of PH-1 (1 mM).

of proteins [46]. Fig. 6 shows the helicity of BSA in the presence of increasing concentration of PH-1. In the wavelength region of 190–260 nm, the CD spectrum of a protein provides information about its conformation in relation to the secondary structure. The binding of PH-1 to BSA changes both these bands and also shifting in the negative minima and results suggest that interaction of PH-1 with BSA may cause some conformational changes of BSA. Similar results were also obtained with PH-2 and PH-3, as shown in Supplementary Fig. 7.

3.7. Energy transfer between BSA and PHs

Förster's resonance energy transfer (FRET) is a distance-dependent interaction between different electronic excited states of molecules. This process allows the excitation energy to be transferred from one molecule (donor) to another molecule (acceptor) without emission of a photon from the former molecular system. This can determine the proximity and relative angular orientation of fluorophores. The donor and acceptor fluorophores can be entirely separated or attached to the same macromolecule. According to FRET theory [47], the rate of energy transfer depends on three factors: (i) the distance between the donor and the acceptor, (ii) the relative orientation of the donor and acceptor dipoles and (iii) the extent of overlap of the emission spectrum of the donor with the absorption spectrum of the acceptor. The energy transfer effect E is also related to the critical energy transfer distance R_0, as described in the following equation.

$$E = 1 - \frac{F}{F_0} = R_0^6/(R_0^6 + r^6) \quad (6)$$

where F and F_0 are the fluorescence intensities of BSA in the presence and absence of PHs, respectively, r is the distance between the acceptor and donor, and R_0 is the critical distance when the transfer efficiency is 50%. R_0 can be determined by the following equation.

$$R_0^6 = 8.8 \times 10^{-25} k^2 N^{-4} \phi J \quad (7)$$

where k^2 is the spatial orientation factor between the emission dipole of the donor and the absorption dipole of the acceptor. The dipole orientation factor (k^2) is the least certain parameter that is used in the calculation of the critical transfer distance. Theoretically, k^2 can range from 0 to 4 and the extreme values require very rigid orientations.

When both the donor and the acceptor tumble rapidly and are free to assume any orientation, k^2 equals 2/3. When only the donor is free to rotate, k^2 can vary from 1/3 to 4/3 [29]. N is the refractive index of the medium, ϕ is the fluorescence quantum yield of the donor, and J is the overlap integral of the fluorescence emission spectrum of the donor. The absorption spectrum of the acceptor is given by the following equation.

$$J = \sum F(\lambda)\varepsilon(\lambda)\lambda^4 \Delta\lambda / \sum F(\lambda)\Delta\lambda \quad (8)$$

where F (λ) is the fluorescence intensity of the fluorescent donor at wavelength λ and is dimensionless, ε (λ) is the molar absorption coefficient of the acceptor at wavelength λ. The overlap of the UV absorption spectra of PH-1 with the fluorescence emission spectra of BSA is shown in Fig. 7. The overlap of the UV absorption spectra of PH-2 and PH-3 emission spectra of BSA is shown in Supplementary Fig. 8.

The values of spatial orientation factor, quantum yield and refractive index for BSA, i.e., k^2=2/3, ϕ=0.15 and N=1.336, have been previously reported [48]. The experimental results of distance parameters are shown in Table 4. The values of r for the compounds are all less than the academic predicted value (7 nm) [49]. Furthermore, the distances obtained by this method agree well with literature values of substrate binding to BSA at site IIA [50].

The average distances between a donor fluorophore and an acceptor fluorophore are within the 2–7 nm range [51–53]. This results in energy transfer between BSA and PHs. This also indicates that the fluorescence quenching of BSA is a non-radiative transfer process. The binding distance r much less than 7 nm indicates that the energy transfer occurs between BSA and PHs with high probability [49] and also the fluorescence quenching of BSA is a non-radiative transfer process.

3.8. Molecular modeling

The fluorescence, UV–vis, and CD spectroscopic results were complemented by molecular modeling, in which PHs were docked to BSA to determine the preferred binding site and the binding mode. Molecular docking technique was employed to understand different binding modes of BSA-PHs interaction [54–56]. The 3D structure of BSA was obtained from Proteins Data Bank. The possible conformations of the BSA-PH-1 complex were calculated using AutoDock 4.0 program. Out of 10 conformers obtained, the conformer with the lowest binding free energy was used for further analysis. The best

Table 4
The distance parameters between PHs and BSA.

System	J (cm^3×L/mol)	E	R_0 (nm)	r (nm)
BSA-PH-1	9.26×10^{-16}	0.045	1.71	2.86
BSA-PH-2	4.57×10^{-15}	0.14	2.24	3.03
BSA-PH-3	3.68×10^{-14}	0.053	3.17	5.12

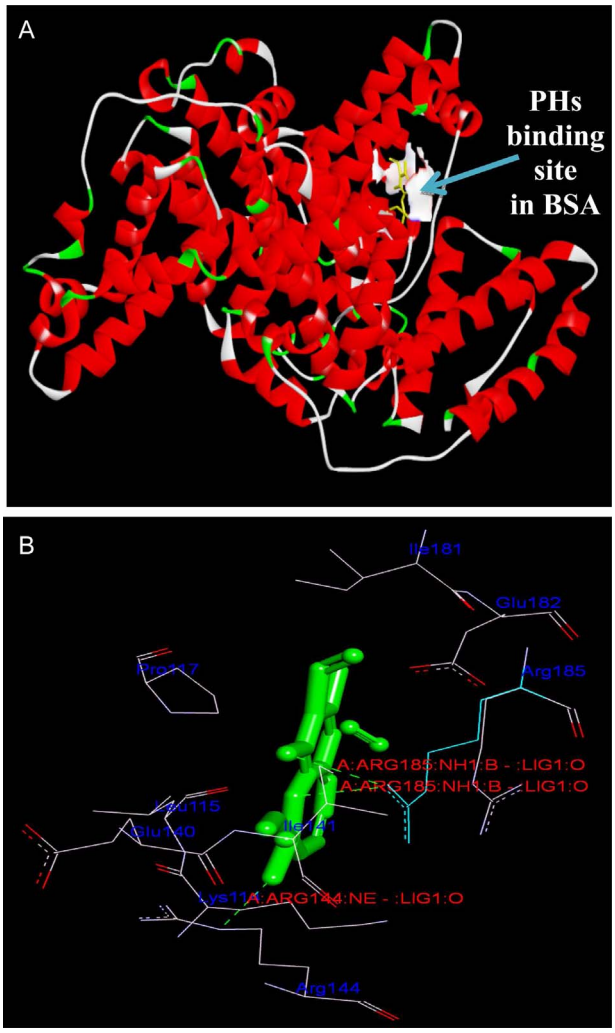

Fig. 8. Docking of PHs with BSA. (A) place of interaction of PH-1 and BSA and (B) the surrounding amino acid residues of BSA within 5 Å from PH-1 (green colored).

energy ranked model (Fig. 8A) revealed that the PH-1 is bound at the interface between two sub-domains IIA and IIIA, which is located just above the entrance of the binding pocket of IIA. PH-1 molecule is surrounded by 9 amino acid residues within 5 Å: 4 hydrophobic residue (ILeu141, Leu115, Pro117, Ile181) and 5 ionic residues (Arg185, Arg144, Glu140, Glu182, Lys114), Moreover, there are three hydrogen bonds between the hydroxyl groups of PH-1 and the amino acid residues of BSA; they are Chain A: Arg144:NE-:Lig1O, Chain A: Arg185:NH1:B-:Lig1O and Chain A: Arg185:NH1:B-:Lig1O (Fig. 8B). Docking results of PH-2 and PH-3 are shown in Supplementary Fig. 9.

In case of PH-2, it is surrounded by 10 amino acid residues within 5 Å: 5 hydrophobic residue (ILeu141, Leu115, Pro117, Ile181, Val188), 2 hydrophilic residues (Tyr160, Tyr137) and 3 ionic residues (Arg185, Glu140, Lys136). There are two hydrogen bonds between the hydroxyl groups of PH-2 and the amino acid residues of BSA; they are Chain A: Arg185:NH1: B-:Lig1O and Lig1: O-A: Ile181: O. In case of PH-3, it is surrounded by 8 amino acid residues within 5 Å: 2 hydrophobic residues (Leu115, Pro117), 2 hydrophilic residues (Tyr160, Tyr137) and 4 ionic residues (Arg185, Arg144, Glu182, Lys114) and in this case no H-bond is found. The formation of hydrogen bonds decreases the hydrophilicity and increases the hydrophobicity to stabilize the BSA-PH-1 system. Therefore, it may be concluded that the interaction between PH and BSA is dominated by hydrogen bonds and van der Waals interactions. The experimental results are in well agreement with the results of binding mode study.

4. Conclusion

The interaction of PHs with BSA revealed that the quenching of BSA fluorescence is dynamic quenching, and that van der Waals force and hydrogen bond are the responsible factors for this type of interaction. The binding distances of PHs with BSA were calculated on the basis of the Forster's theory, which indicates that the energy transfer can occur. Moreover, molecular docking study confirms the interaction between the PHs and BSA , which is consistent with the reported data. This study provides important insights into the interactions of the physiologically important proteins BSA with PHs.

Acknowledgments

Swarup Roy is thankful to the Department of Science and Technology (DST, New Delhi), for a DST INSPIRE fellowship (IF 110421). Raj Kumar Nandi and Sintu Ganai thanks CSIR (New Delhi) for their research fellowships.

Appendix A. Supplementary material

Supplementary data associated with this article can be found in the online version at http://dx.doi.org/10.1016/j.jpha.2016.05.009.

References

[1] D.C. Carter, J.X. Ho, Structure of serum albumin, Adv. Protein Chem. 45 (1994) 153–203.
[2] U. Mathias, M. Jung, Determination of drug-serum protein interactions via fluorescence polarization measurements, Anal. Bioanal. Chem. 388 (2007) 1147–1156.
[3] P. Bourasssa, C.D. Kanakis, P. Tarantilis, et al., Resveratrol, genistein, and curcumin bind bovine serum albumin, J. Phys. Chem. B 114 (2010) 3348–3354.
[4] A.B. Smith, C.M. Taylor, S.J. Benkovic, et al., Peptide bond formation via catalytic antibodies: synthesis of a novel phosphonate diester hapten, Tetrahedron Lett. 35 (1994) 6853–6856.
[5] I. Morita, K. Kunimoto, M. Tsuda, et al., Synthesis and antihypertensive activities of 1,4-dihydropyridine-5-phosphonate derivatives, Chem. Pharm. Bull. 35 (1987) 4144–4154.
[6] Y. Zu, L. Meng, X. Zhao, et al., Preparation of 10-hydroxycamptothecin-loaded glycyrrhizic acid-conjugated bovine serum albumin nanoparticles for hepatocellular carcinoma-targeted drug delivery, Int. J. Nanomed. 8 (2013) 1207–1222.
[7] X. Yu, Z. Liao, Q. Yao, et al., The investigation of the interaction between tropicamide and bovine serum albumin by spectroscopic methods, Spectrochim. Acta A 118 (2014) 331–336.
[8] B. Mondal, B. Sena, E. Zangrando, et al., A dysprosium-based metalorganic framework: Synthesis,characterization, crystal structure and interaction with calf thymus-DNA and bovine serum albumin, J. Chem. Sci. 126 (2014) 1115–1124.
[9] X. Zhang, R. Gao, D. Li, et al., Study on interaction between 5-bromo-4-thio-2′-deoxyuridine and human serum albumin by spectroscopy and molecular docking, Spectrochim. Acta A 136 (2015) 1775–1781.
[10] X. Yu, Z. Liao, B. Jiang, et al., Spectroscopic analyses on interaction of bovine serum albumin with novel spiro[cyclopropane-pyrrolizin], Spectrochim. Acta A 137 (2015) 129–136.
[11] Q. Wang, S. Zhang, Studies of interaction between clenbuterol hydrochloride and two serum albumins by multispectroscopic approaches in vitro, Luminescence 29 (2014) 492–499.
[12] M. Toprak, M. Arık, The investigation of the interaction between orientin and bovine serum albumin by spectroscopic analysis, Luminescence 29 (2014) 805–809.
[13] S. Roy, S. Ponra, R.K. Nandi, et al., Biophysical study on the interaction of spirooxindole-annulated thiopyran derivatives with bovine serum albumin using spectroscopic and docking methods, Adv. Mater. Lett. 6 (2015) 913–919.
[14] S. Roy, S. Ponra, T. Ghosh, et al., Combined spectroscopic and molecular docking study of binding interaction of pyrano[3, 2-f]quinoline derivatives with bovine serum albumins and its application in mammalian cell imaging, Adv. Mater. Lett. 6 (2015) 1004–1011.
[15] S. Roy, S. Ganai, R.K. Nandi, et al., Studies of the interaction of bovine serum albumin with pyrimidine-annulated spiro-dihydrofuran and its biological activities, Adv. Mater. Lett. 6 (2015) 1018–1024.
[16] Q. Yao, X. Yu, T. Zheng, et al., Spectroscopic studies on the interaction of carteolol hydrochloride and urea-induced bovine serum albumin, Spectrochim. Acta A 113 (2013) 447–451.
[17] X. Yu, Z. Liao, Q. Yao, et al., Spectroscopic studies on the interaction of Phacolysin and bovine serum albumin, Spectrochim. Acta A 127 (2014) 231–236.
[18] Y.-J. Hu, Y. Liu, X.-S. Shen, et al., Studies on the interaction between 1-hexylcarbamoyl-5-fluorouracil and bovine serum albumin, J. Mol. Struct. 738 (2005) 143–147.

[19] L. Zhang, B. Liu, Z. Li, et al., Comparative studies on the interaction of cefixime with bovine serum albumin by fluorescence quenching spectroscopy and synchronous fluorescence spectroscopy, Luminescence 30 (2015) 686–692.
[20] S.K. Dutta, S.K. Basu, K.K. Sen, Binding of diclofenac sodium with bovine serum albumin at different temperatures, pH and ionic strengths, Indian J. Exp. Biol. 44 (2006) 123–127.
[21] N. Wang, L. Ye, B.Q. Zhao, et al., Spectroscopic studies on the interaction of efonidipine with bovine serum albumin, Braz. J. Med. Biol. Res. 41 (2008) 589–595.
[22] S. Nafisi, G.B. Sadeghi, A. PanahYab, Interaction of aspirin and vitamin C with bovine serum albumin, J. Photochem. Photobiol. B 105 (2011) 198–202.
[23] K.C. Majumdar, R.K. Nandi, S. Ganai, Synthesis of phosphorus containing medium ring heterocycles by sequential Claisen rearrangement and ring closing metathesis, Tetrahedron Lett. 55 (2014) 1247–1250.
[24] J.J. Stephanos, Drug-protein interactions: two-site binding of heterocyclic ligands to monomeric hemoglobin, J. Inorg. Biochem. 62 (1996) 155–169.
[25] H.A. Benesi, J.H. Hildebrand, Spectrophotometric investigation of the interaction of iodine with aromatic hydrocarbons, J. Am. Chem. Soc. 71 (1949) 2703–2707.
[26] A. Sharma, S.G. Schulman, Introduction to Fluorescence Spectroscopy, Wiley Press, New York, 1999.
[27] A. Sulkowska, Interaction of drug with bovine and human serum albumin, J. Mol. Struct. 614 (2002) 227–232.
[28] M.A. Jhonsi, A. Kathiravan, R. Renganathan, Spectroscopic studies on the interaction of colloidal capped CdS nanoparticles with bovine serum albumin, Colloids Surf. B 72 (2009) 167–172.
[29] J.R. Lakowicz, Principle of Fluorescence Spectroscopy, Springer, New York, 1999.
[30] R. Wang, Y. Chai, R. Wang, et al., Study of the interaction between bovine serum albumin and analogs of by biphenyldicarboxylate spectrofluorimetry, Spectrochim. Acta A 96 (2012) 324–331.
[31] S. Roy, T.K. Das, Spectroscopic studies of interaction between biologically synthesized silver nanoparticles and bovine serum albumin, J. Nanosci. Nanotechnol. 14 (2014) 4899–4905.
[32] Y. Shi, H. Liu, M. Xu, et al., Spectroscopic studies on the interaction between an anticancer drug ampelopsin and bovine serum albumin, Spectrochim. Acta A 87 (2012) 251–257.
[33] S. Roy, T.K. Das, Investigation of interaction between casein enzyme hydrolysate and biosynthesized silver nanoparticles by spectroscopy, Nanosci. Nanotechnol. Lett. 6 (2014) 547–554.
[34] M.X. Xie, M. Long, Y. Liu, et al., Characterization of the interaction between human serum albumin and morin, Biochim. Biophys. Acta 2006 (1760) 1184–1191.
[35] I.M. Klotz, Physiochemical aspects of drug-protein interactions: a general perspective, Ann. N.Y. Acad. Sci. 226 (1993) 18–35.
[36] Y. Liua, M. Chenb, Z. Luoa, et al., Investigation on the site-selective binding of bovine serum albumin by erlotinib hydrochloride, J. Biomol. Struct. Dyn. 31 (2013) 1160–1174.
[37] Y.-J. Hu, Y. Liu, X.-H. Xiao, Investigation of the interaction between berberine and human serum albumin, Biomacromolecules 10 (2009) 517–521.
[38] D.P. Ross, S. Subramanian, Thermodynamics of protein association reactions: forces contributing to stability, Biochemistry 20 (1981) 3096–3102.
[39] G. Neméthy, H.A. Scheraga, Self-association of insulin and the role of hydrophobic bonding: a thermodynamic model of insulin dimerization, J. Phys. Chem. 66 (1962) 1773–1789.
[40] R. Wangn, H. Dou, Y. Yin, et al., Investigation of the interaction between isomeric derivatives and human serum albumin by fluorescence spectroscopy and molecular modeling, J. Lumin. 154 (2014) 8–14.
[41] C. Xu, J. Gu, X. Ma, et al., Investigation on the interaction of pyrene with bovine serum albumin using spectroscopic methods, Spectrochim. Acta A 125 (2014) 391–395.
[42] Y.-J. Hu, Y. Liu, Z.-B. Pi, et al., Interaction of cromolyn sodium with human serum albumin: a fluorescence quenching study, Bioorg. Med. Chem. 13 (2005) 6609–6614.
[43] J.N. Miller, Recent advances in molecular luminescence analysis, Proc. Anal. Div. Chem. Soc. 16 (1979) 203–208.
[44] K.M. Naik, D.B. Kolli, S.T. Nandibewoor, Elucidation of binding mechanism of hydroxyurea on serum albumins by different spectroscopic studies, Springerplus 3 (2014) 1–13.
[45] Y. Zhang, B. Zhou, Y. Liu, et al., Fluorescence study on the interaction of bovine serum albumin with p-aminoazobenzene, J. Fluoresc. 18 (2008) 109–118.
[46] Y.J. Hu, Y. Liu, X.S. Shen, et al., Studies on the interaction between 1-hexylcarbamoyl-5-fluorouracil and bovine serum albumin, J. Mol. Struct. 738 (2005) 143–147.
[47] T. Förster, Modern Quantum Chemistry, Academic, New York, 1996.
[48] L. Cyril, J.K. Earl, W.M. Sperry, Biochemist's Handbook, E. & F.N. Spon, London, 1961.
[49] B. Valeur, J.C. Brochon, New trends in fluorescence spectroscopy, Springer, Berlin, 2001.
[50] S. Deepa, A.K. Mishra, Fluorescence spectroscopic study of serum albumin-bromadiolone interaction: fluorimetric determination of bromadiolone, J. Pharm. Biomed. Anal. 38 (2005) 556–563.
[51] S. Weiss, Fluorescence spectroscopy of single biomolecules, Science 283 (1999) 1676–1683.
[52] S. Roy, T.K. Das, Effect of silver nanoparticles on vitamin C by analyzing the change of photoluminescence spectrum of vitamin C, Adv. Sci. Eng. Med. 6 (2014) 1105–1110.
[53] S. Roy, T.K. Das, Study of interaction between Tryptophan, Tyrosine and Phenylalanine separately with silver nanoparticles by fluorescence quenching method, J. Appl. Spectrosc. 82 (2015) 598–606.
[54] W.H. Gao, N. Li, Y.W. Chen, et al., Study of interaction between syringin and human serum albumin by multi-spectroscopic method and atomic force microscopy, J. Mol. Struct. 983 (2010) 133–140.
[55] K. Paal, A. Shkarupin, L. Beckford, Paclitaxel binding to human serum albumin-automated docking studies, Bioorg. Med. Chem. 15 (2007) 1323–1329.
[56] M.D. Meti, S.T. Nandibewoor, S.D. Joshi, et al., Multi-spectroscopic investigation of the binding interaction of fosfomycin with bovine serum albumin, J. Pharm. Anal. 5 (2015) 249–255.